Sliding Mode Controller with Sliding Perturbation Observer Based on Gain Optimization using Genetic Algorithm

Ki Sung You
Graduate School, Department of Mechanical and Intelligent Systems Engineering, Pusan National University, Busan 609-735, Korea
Min Cheol Lee*, Wan Suk Yoo
School of Mechanical Engineering and Research Institute of Mechanical Technology, Pusan National University, San 30, Changjeon-dong, Keumjeong-gu, Busan 609-735, Korea

The Stewart platform manipulator is a closed-kinematics chain robot manipulator that is capable of providing high structural rigidity and positional accuracy. However, this is a complex and nonlinear system, so the control performance of the system is not so good. In this paper, a new robust motion control algorithm is proposed. The algorithm uses partial state feedback for a class of nonlinear systems with modeling uncertainties and external disturbances. The major contribution is the design of a robust observer for the state and the perturbation of the Stewart platform, which is combined with a variable structure controller (VSC). The combination of controller and observer provides the robust routine called sliding mode control with sliding perturbation observer (SMCSPO). The optimal gains of SMCSPO, which is determined by nominal eigenvalues, are easily obtained by genetic algorithm. The proposed fitness function that evaluates the gain optimization is to put sliding function. The control performance of the proposed algorithm is evaluated by the simulation and experiment to apply to the Stewart platform. The results showed high accuracy and good performance.

Key Words : Sliding Perturbation Observer, Sliding Mode Control, Genetic Algorithm, Gain Optimization

1. Introduction

The Stewart platform manipulator is the manipulator that has the closed-loop structure with an upper plate of end-effector and a lower plate of base frame (Stewart, 1966). The Stewart platform manipulator has the merit with high working accuracy and rigid stiffness compared with a serial one. However, this has a complex structure, so a control performance of the system is not so good (Hashimoto et al., 1987).

The major contribution of the design of robust controller for the Stewart platform manipulator introduces the development and design of robust observer for the state and the perturbation which is integrated into a variable structure controller structure (Slotine et al., 1987). The combination of controller and observer gives rise to the robust routine called sliding mode control with sliding perturbation observer. Sliding observer is a high performance state estimator well suited for nonlinear uncertain systems with partial state feedback (Elmali and Olgac, 1992). Then system is not required additional sensor. The sliding function of this observer consists of the estimation error of the available output. The sliding observer doesn't need a full state feedback in the perturbation estimation and reduces the implemen-

* Corresponding Author,
E-mail : mclee@pusan.ac.kr
TEL : +82-51-510-2439; **FAX** : +82-51-512-9835
School of Mechanical Engineering and Research Institute of Mechanical Technology, Pusan National University, San 30, Changjeon-dong, Keumjeong-gu, Busan 609-735, Korea. (Manuscript **Received** September 19, 2003; **Revised** January 5, 2004)

tation costs (Slotine et al., 1987). The combined observer which is able to provide much better state estimation accuracy is named sliding perturbation observer (SPO) (Terra and Olgac, 1997). The combination of this SPO and sliding mode controller (SMC) results in a high performance algorithm that is robust against perturbations, utilizes only partial state feedback.

In this paper, a new robust motion control algorithm using partial state feedback for a class of nonlinear systems with modeling uncertainties and external disturbances is proposed. The algorithm is applied to the Stewart platform to evaluate the control performance. The optimal gains of the motion control algorithm are easily obtained by genetic algorithm.

This paper is organized as follows: In Section 2, design of sliding perturbation observer is introduced. In Section 3, composition of controller and algorithm for selecting robust control gain is proposed. In Section 4, the proposed approach is evaluated through simulation and experiment. This paper concludes in Section 5.

2. Design of Sliding Perturbation Observer

This section describes the proposed perturbation observer without considering the closed-loop control. The developed Stewart platform for a vehicle simulator is shown in Fig. 1.

Fig. 1 The Stewart platform for a vehicle driving simulator

2.1 Definition of perturbation

Generally, the governing equation of the "j"-th actuator with n-degree of freedom is defined as

$$\ddot{x}_j = f_j(\boldsymbol{x}) + \Delta f_j(\boldsymbol{x}) + \sum_{i=1}^{n}[(b_{ji}(\boldsymbol{x}) + \Delta b_{ji}(\boldsymbol{x}))\,u_i] + d_j(t),\ (j=1, \cdots, n) \quad (1)$$

where

$\boldsymbol{x} \equiv [X_1, \cdots, X_n]^T$: state vector
$X_j \equiv [x_j\ \dot{x}_j]^T$: state variable
$\Delta f_j(\boldsymbol{x})$: uncertainties of nonlinear driving terms
$\Delta b_{ji}(\boldsymbol{x})$: uncertainties of the control gain matrix
$d_j(t)$: external disturbance
u_i : control input
$f_j,\ b_{ji}$: continuous functions of state
"i" : symbol which represents elements of control gain matrix effected by control input.

In the governing equation, perturbation is defined as the combination of all the uncertainties and nonlinear term of Eq. (1).

$$\Psi_j(\boldsymbol{x},\ t) = \Delta f_j(\boldsymbol{x}) + \sum_{i=1}^{n}[\Delta b_{ji}(\boldsymbol{x})\,u_i] + d_j(t) \quad (2)$$

The control task is to derive the state $\boldsymbol{x}$ toward a desired state $\boldsymbol{x}_d \equiv [X_{1d} \cdots X_{nd}]^T$ in spite of these perturbations (Elmali and Olgac, 1992). It is assumed that the perturbations are upper bounded by a known continuous function of the state:

$$\Gamma_j(\boldsymbol{x},\ t) = F_j(\boldsymbol{x}) + \sum_{i=1}^{n}|\ \Phi_{ji}(\boldsymbol{x})\,u_i\ | + D_j(t) > |\ \Psi_j(t)\ | \quad (3)$$

where $F_j > |\ \Delta f_j\ |$, $\Phi_{ji} > |\ \Delta b_{ji}\ |$, $D_j > |\ d_j\ |$ represent the expected upper bounds of the uncertainties, respectively.

2.2 Sliding perturbation observer

Sliding perturbation observer is the combination of a perturbation observer and sliding observer, which results in a more effective observer structure. Before integrating SPO into SMC, it is convenient to decouple the control variable using

the following transformation. The new control variable which is used in order to decouple the control of Eq. (1) is defined as

$$f_j(\hat{\boldsymbol{x}})+\sum_{i=1}^{n} b_{ji}(\hat{\boldsymbol{x}})\, u_i=\alpha_{3j}\bar{u}_j \tag{4}$$

where $\hat{\boldsymbol{x}}$ is the estimated state vector, α_{3j} is an arbitrary positive number and $\bar{u}_j$ is the new control variable (Terra and Olgac, 1997). Throughout the text, " $\tilde{}$ ", refers to estimation errors whereas " $\hat{}$ " symbolizes the estimated quantity. The original control vector of Eq. (1) is obtained as

$$\boldsymbol{u}=\boldsymbol{B}^{-1}Col[\alpha_{3j}\bar{u}_j-f_j(\hat{\boldsymbol{x}})] \tag{5}$$

where $\boldsymbol{u}=[u_1, \cdots, u_n]^T$ and $\boldsymbol{B}=[b_{ji}(\hat{\boldsymbol{x}})]_{n\times n}$.

Transformation of Eq. (4) simply allows us to write the system dynamics. The state representation of the simplified dynamics is given by

$$\dot{x}_{1j}=x_{2j} \tag{6a}$$

$$\dot{x}_{2j}=\alpha_{3j}\bar{u}_j+\Psi_j \tag{6b}$$

$$y_j=x_{1j} \tag{6c}$$

where "j" is the number of hydraulic actuators.

Let x_{3j} be a new state variable defined as

$$x_{3j}=\alpha_{3j}x_{2j}-\Psi_j/\alpha_{3j} \tag{7}$$

It is desirable to observe the variable x_{3j} and consequently calculate Ψ_j using Eq. (7) instead of estimating them directly. In order to accomplish this, it is assumed that

(1) the time derivative of Ψ_j exists (i.e., there are only continuous perturbations) and is bounded,

(2) the spectrum of Ψ_j lies within a known finite frequency range.

Note that the assumption 1 can not hold at the instant of discontinuities in the perturbation signal (e.g., dry friction at zero velocity point).

The structure of the sliding perturbation observer consists of the perturbation observer and sliding one. The sliding perturbation observer utilizes only partial state feedback (x_{1j} in this treatment). Consequently, it is necessary to estimate x_{2j} in order to obtain the estimated perturbation $\hat{\Psi}_j$. The sliding perturbation observer is better than the general perturbation observer because this observer can provide an on-line perturbation estimation scheme using only partial state feedback. The estimation accuracy of x_{2j} improves at least to the order of the perturbation estimation accuracy. This structure (Slotine et al., 1987) can be achieved by writing the observer equation as

$$\dot{\hat{x}}_{1j}=\hat{x}_{2j}-k_{1j}sat(\tilde{x}_{1j})-\alpha_{1j}\tilde{x}_{1j} \tag{8a}$$

$$\dot{\hat{x}}_{2j}=\alpha_{3j}\bar{u}_j-k_{2j}sat(\tilde{x}_{1j})-\alpha_{2j}\tilde{x}_{1j}+\hat{\Psi}_j \tag{8b}$$

$$\dot{\hat{x}}_{3j}=\alpha_{3j}^2(-\hat{x}_{3j}+\alpha_{3j}\hat{x}_{2j}+\bar{u}_j) \tag{8c}$$

where $\hat{\Psi}_j$ is derived as

$$\hat{\Psi}_j=\alpha_{3j}(-\hat{x}_{3j}+\alpha_{3j}\hat{x}_{2j}) \tag{9}$$

k_{1j}, k_{2j}, α_{1j}, α_{2j} are positive numbers, $\tilde{x}_{1j}=\hat{x}_{1j}-x_{1j}$ is the estimation error of the measurable state, and $sat(\tilde{x}_{1j})$ is the saturation function for the existence of sliding mode.

3. Composition of Controller and Gain Optimization of SMCSPO

3.1 Design procedure

As integrating SMC law and SPO scheme, SMCSPO of robust nonlinear controller is strong against perturbations. For the system of Eq. (6), we define the estimated sliding function as

$$\hat{s}_j=\dot{\hat{e}}_j+c_{j1}\hat{e}_j \tag{10}$$

where $c_{j1}(>0)$ is a slope of switching line and $\hat{e}_j(=\hat{x}_{1j}-x_{1dj})$ is the estimated position tracking error. $[x_{1dj}\ \dot{x}_{1dj}]^T$ is the desired states for the motion of the Stewart platform. The control $\bar{u}_j$ is selected to enforce $\dot{\hat{s}}_j\hat{s}_j<0$ outside a prescribed manifold. A desired $\dot{\hat{s}}_j$ is selected as

$$\dot{\hat{s}}_j=-K_j\, sat(\hat{s}_j) \tag{11}$$

where

$$sat(\hat{s}_j)=\begin{cases}\hat{s}_j/|\hat{s}_j|, & \text{if } |\hat{s}_j|\geq\varepsilon_{sj}\\ \hat{s}_j/\varepsilon_{sj}, & \text{if } |\hat{s}_j|\leq\varepsilon_{sj}\end{cases} \tag{12}$$

is used due to its desirable anti-chatter properties and $K_j(K_j>0)$ is the robust control gain. In this equation, ε_{sj} represents the width of boundary

layer of the SMC, which is different value with the boundary layer ε_{oj} in SPO.

Using Eq. (8), Eq. (9), Eq. (10), Eq. (11), and Eq. (12) it is possible to compute $\dot{\hat{s}}_j$ as

$$\dot{\hat{s}}_j=\alpha_{3j}\bar{u}_j-[k_{2j}/\varepsilon_{oj}+c_{j1}(k_{1j}/\varepsilon_{oj})-(k_{1j}/\varepsilon_{oj})^2]\tilde{x}_{1j} +\ddot{x}_{1dj}+c_{j1}(\hat{x}_{2j}-\dot{x}_{1dj})+\hat{\Psi}_j \quad (13)$$

The resulting $|\hat{s}_j|$-dynamics including the effects of $\tilde{x}_{2j}$ is selected as

$$\dot{\hat{s}}_j=-K_j\, sat(\hat{s}_j)-(k_{1j}/\varepsilon_{oj})\tilde{x}_{2j} \quad (14)$$

In order to enforce Eq. (11) when $\tilde{x}_{2j}=0$, a control law is selected as

$$\bar{u}_j=\frac{1}{\alpha_{3j}}\{-K_j\, sat(\hat{s}_j)-(k_{1j}/\varepsilon_{oj})\tilde{x}_{2j} +[k_{2j}/\varepsilon_{oj}+c_{j1}(k_{1j}/\varepsilon_{oj})-(k_{1j}/\varepsilon_{oj})^2]\tilde{x}_{1j} +\ddot{x}_{1di}-c_{j1}(\hat{x}_{2j}-\dot{x}_{1di})-\beta_j\hat{\Psi}_j\} \quad (15)$$

where β_j is positive gain of perturbation and $\beta_j\hat{\Psi}_j$ is upper bounded by a known continuous function of the state such as Eq. (3).

The conditions for the existence of sliding mode are given by

$$sat(\tilde{x}_{1j})=\begin{cases}\tilde{x}_{1j}/|\tilde{x}_{1j}|, & \text{if } |\tilde{x}_{1j}|\geq\varepsilon_{oj}\\ \tilde{x}_{1j}\varepsilon_{oj}, & \text{if } |\tilde{x}_{1j}|\leq\varepsilon_{oj}\end{cases} \quad (16)$$

where ε_{oj} is the boundary layer of the sliding perturbation observer.

The observer's sliding mode takes place on the line $\tilde{x}_{1j}=0$ of the observer state space $\tilde{x}_{1j}$ vs $\tilde{x}_{2j}$. Fig. 2 depicts a typical state space trajectory. The condition for the existence of sliding mode are

$$\tilde{x}_2\leq\alpha_1\tilde{x}_1+k_1 \quad (\text{if } \tilde{x}_1>0) \quad (17a)$$

$$\tilde{x}_2\geq\alpha_1\tilde{x}_1-k_1 \quad (\text{if } \tilde{x}_1<0) \quad (17b)$$

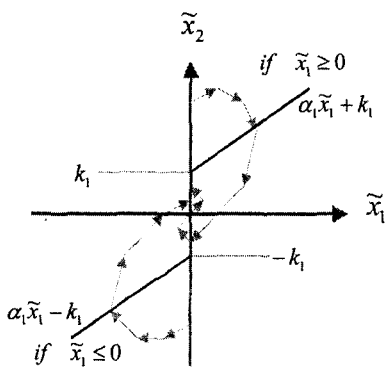

Fig. 2 Observer state space and sliding mode

From the sliding condition Eq. (16), the state estimation error is bounded by $|\tilde{x}_{2j}|\leq k_{1j}$. Therefore, in order to satisfy $\dot{\hat{s}}_j\hat{s}<0$ outside the manifold $|\hat{s}_j|\leq\varepsilon_{oj}$, the robust control gains must be chosen such as $K_j\geq k_{1j}^2/\varepsilon_{oj}$.

A systematic general design procedure considering the hardware limitations of the system describe by the fact that the eigenvalue of the characteristic equation of systematic matrix of observer and s_j dynamics is negative real number. For simplicity, all the desired poles are selected to be the same real valued location $\lambda=-\lambda_d(\lambda_d>0)$. This leads to the following design solution.

$$\frac{k_{1j}}{\varepsilon_{oj}}=3\lambda_d,\ \frac{k_{2j}}{k_{1j}}=\lambda_d,\ \alpha_{3j}=\sqrt{\frac{\lambda_d}{3}},\quad c_{j1}=K_j/\varepsilon_{oj}=\lambda_d \quad (18)$$

Physical limitations of the control system define the optimum placement of λ_d. The λ_d is effected by hardware constraints such as sampling frequency, dominant time delay, measurement delay and actuator dynamics.

3.2 Gain optimization using genetic algorithm

To evaluate the designed observer performance in frequency domain, the magnitude plots of SPO and sliding observer (SO) when perturbation occurs in system are compared as shown in Fig. 3. SPO clearly yields higher attenuation up to approximately $\omega/\lambda_d=0.4$. This means better estimation accuracy within this normalized value

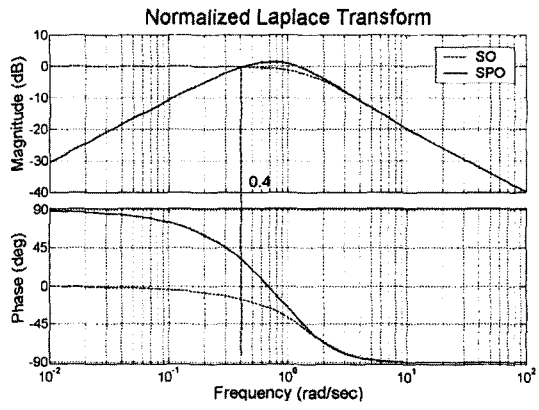

Fig. 3 Bode plots of SPO and SO

frequency. The magnitude plots of $s_j(p)/\Psi_j(p)$ for SMC and SMCSPO with perturbation are compared as shown in Fig. 4. For high frequency contents of Ψ_j, both algorithms produce the same result. In the mid-frequency range, the maximum discrepancy is about 10 dB in favor of SMC. In the lower frequency rangl, however, SMCSPO performs better than SMC up to a selected frequency λ_Ψ equal to $0.1\lambda_d$, which should be set higher value than the expected perturbation frequencies so that the attenuation rate of SMCSPO may be larger than that of SMC. It is important to note that the SMC does not reguire full state feedback. There is no measurement noise in SMCSPO because chattering is reduced. The selection of optimal placement of λ_d is very hard due to physical limitations of the control system.

In this paper, the optimal gain λ_d is selected by the genetic algorithm. The scheme of the genetic algorithm is shown in Fig. 5. This algorithm searches the robust control gain using the principles of natural selection. The objective function to optimize the gain consists of the estimated sliding function. The error function and fitness function are given by

$$S_e=\sum_{t=0}^{t_f}\left(\sum_{i=1}^{6}|\hat{s}_i(t)|\right) \tag{19}$$

$$f_{GA}=\frac{W}{1+S_e} \tag{20}$$

where $\hat{s}(t)$ is the estimated sliding function for each sampling time, W is the weighting factor, and error function is the sum of the absolute value that calculated sliding function. This function has an effect on optimizing by the velocity and position errors. As the value of error function is reduced, the fitness function is to reach the maximum fitness. The number of generation is 500. The slope of sliding surface is selected by 21.43.

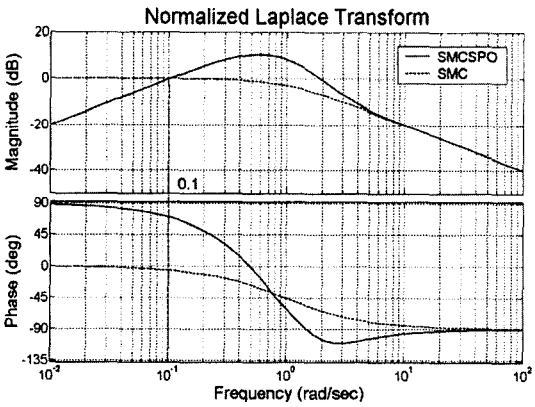

Fig. 4 Bode plots of SMC and SMCSPO

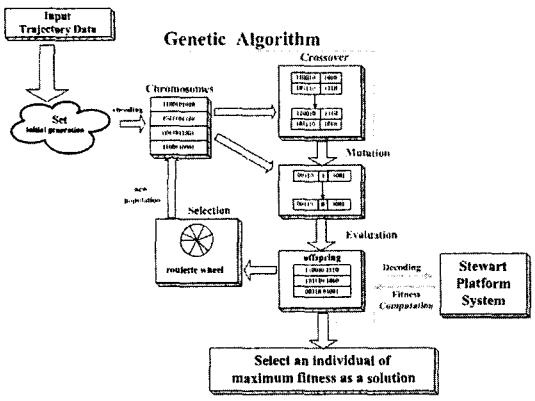

Fig. 5 The scheme of the genetic algorithm

4. Simulation and Experiment

4.1 Modeling of Stewart platform

The dynamic equation of the Stewart platform considering all inertia effect is known to be very difficult to derive. Lebret derived the dynamic equation using the Lagrange method and virtual work principle (Park and Lee, 2002). This equation is written as

$$M_P(q)\ddot{q}+C_P(q,\dot{q})\dot{q}+G_P(q)=J^TU_P \tag{21}$$

where $q=[x, y, z, \alpha, \beta, \gamma]$ is coordinates vector of the upper centroid and α, β, γ are the rotational angles about the x, y, z axes. $M_P(q)\in R^{6\times6}$ is the inertia matrix, $C_P(q)\in R^{6\times6}$ corresponds to the centrifugal and Coriolis forces matrix, $G_P(q)\in R^{6\times1}$ is the gravity force vector, $J(q)\in R^{6\times6}$ is Jacobian matrix, and $U_P(q)\in R^{6\times1}$ is cylinder force vector. After some algebraic operation ($\dot{l}=J\dot{q}$) and kinematic transformation, Eq. (21) can be expressed as

$$\tilde{M}_P(q)\ddot{l}+\tilde{S}_P(q,\dot{q})\dot{l}+\tilde{G}_P(q)=U_P \tag{22}$$

where $l=[l_1, l_2, l_3, l_4, l_5, l_6]$ is cylinder length vector and

$$\tilde{M}_P(q) = J^{-T}(q) M(q) J^{-1}(q)$$

$$\tilde{C}_P(q, \dot{q}) = J^{-T}(q) M(q) \frac{d}{dt} J^{-1}(q) + J^{-T}(q) C(q, \dot{q}) J^{-1}(q)$$

$$\tilde{G}_P(q) = J^{-T}(q) G(q)$$

The cylinder dynamic equation is high order nonlinear equation. If it is assumed that nonlinear part acts as a disturbance to the model, simple linear dynamics is obtained as

$$M_A \ddot{l} + C_A \dot{l} + U_P = K_{SV} U_A \tag{23}$$

where M_A is the summation of equivalent masses of all the translational part in the cylinder, C_A is the equivalent damping coefficient, and K_{SV} is a spool constant. Therefore, the complete nominal dynamic equation of the Stewart platform system including the manipulator and cylinder dynamics is derived as

$$M_T(q) \ddot{l} + C_T(q, \dot{q}) \dot{l} + G_T(q) = K_{SV} U_A \tag{24}$$

where $M_T = \tilde{M}_P + M_A$, $C_T = \tilde{C}_P + C_A$, $G_T = \tilde{G}_P(q)$. After separating linear element and nonlinear element in Eq. (23), this equation can be re-expressed as

$$M_{TL} \ddot{l} + C_{TL} \dot{l} + F = K_{SV} U_A \tag{25}$$

where M_{TL} and C_{TL} is the summation of all linear terms in M_T and C_T. The disturbance term F is the summation of the nonlinear terms of inertia moments, the Coriolis and centrifugal force, the gravity force, and the friction force. The unknown parameters M_{TL} and C_{TL} are estimated by the signal compression method which is used to get equivalent impulse response (Park and Lee, 2002). The estimated parameters are listed in Table 1.

4.2 Simulation

Fig. 6 is the reference trajectory of the Stewart platform. The motion of the platform is composed of the combination of roll and translation. The linear model of hydraulic actuator is derived as

$$\dot{x}_{1j} = x_{2j}$$
$$\dot{x}_{2j} = -\frac{B_{eq}}{M_{eq}} x_{2j} + \frac{K_{sv}}{M_{eq}} u_j \tag{26}$$

Table 1 Estimation results for the Stewart platform

Cylinder No.	Direction	ω_n, ζ	M_{TL}(kg), C_{TL}
1	expansion	16.0, 0.7	90.8, 2034.1
	retraction	13.0, 0.8	91.7, 2024.8
2	expansion	15.0, 0.7	103.3, 2169.7
	retraction	13.0, 0.8	91.7, 2024.4
3	expansion	15.0, 0.7	103.3, 2169, 7
	retraction	14.0, 0.7	79.1, 1771.3
4	expansion	15.0, 0.7	103.3, 2169.7
	retraction	14.5, 0.8	73.7, 2024.4
5	expansion	15.5, 0.7	96.8, 2099.7
	retraction	14.5, 0.8	85.0, 1959.1
6	expansion	15.0, 0.7	103.3, 2169.7
	retraction	13.0, 0.8	91.7, 2024.8

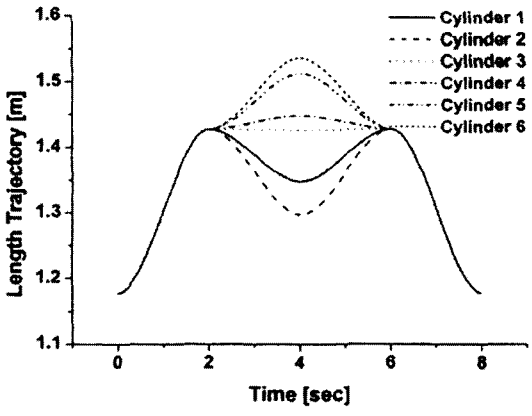

(a) Reference trajectory for position

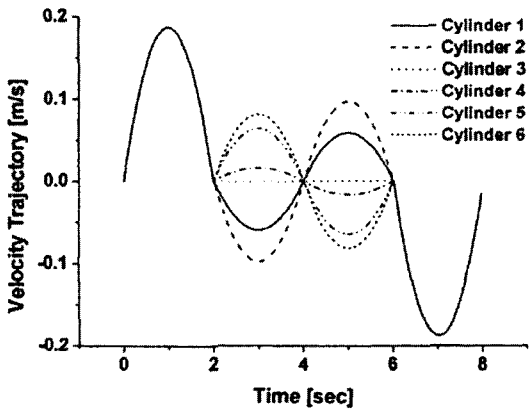

(b) Reference trajectory for velocity

Fig. 6 Reference trajectory

where K_{sv} is the constant of spool, $[x_1\ x_2]$ is the state vector of hydraulic cylinder's rod, B_{eq} and M_{eq} are the equivalent viscosity and the equivalent mass, respectively. The control loop is closed at 100 Hz sampling rate as well. It is assumed that the sampling period is dominant time delay of the closed loop system. In the result of simulation, it is shown that the control performance is so

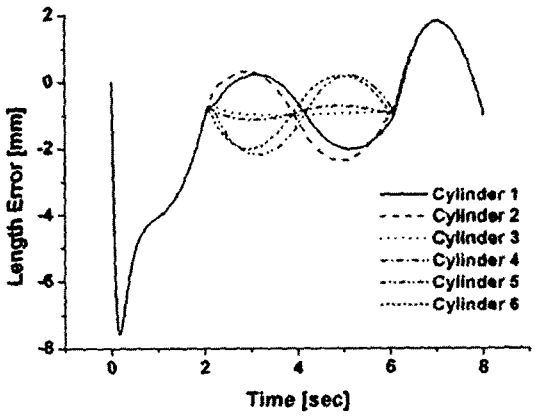

(a) Position tracking error

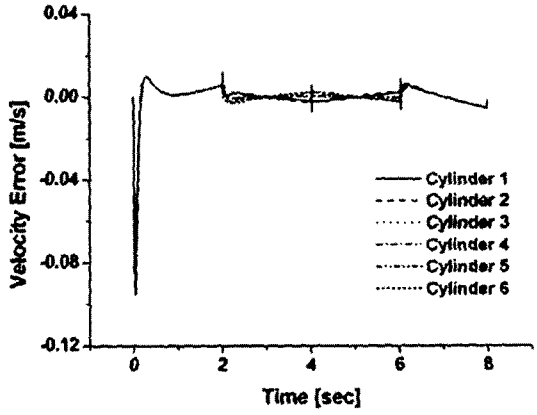

(b) Velocity tracking error

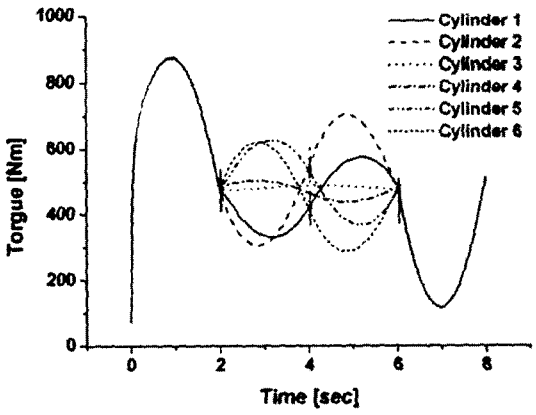

(c) Input torque of the system

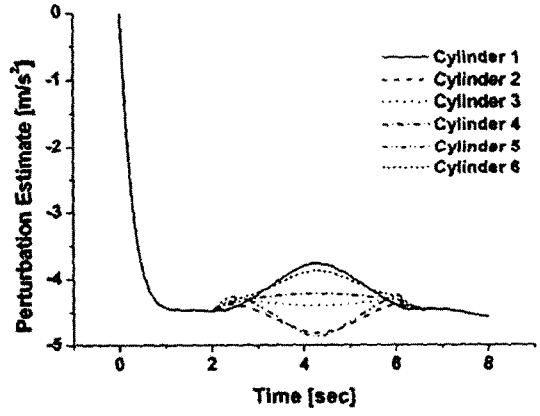

(d) Perturbation estimate

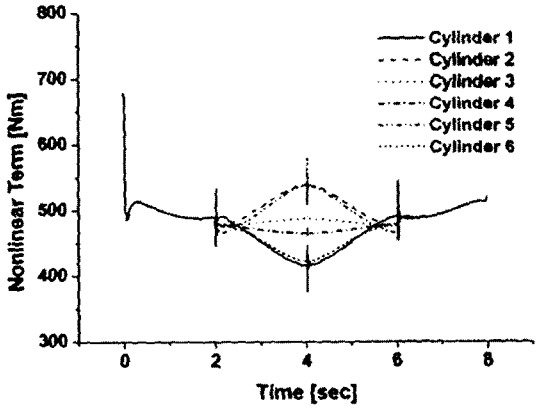

(e) Actual nonlinear term of the system

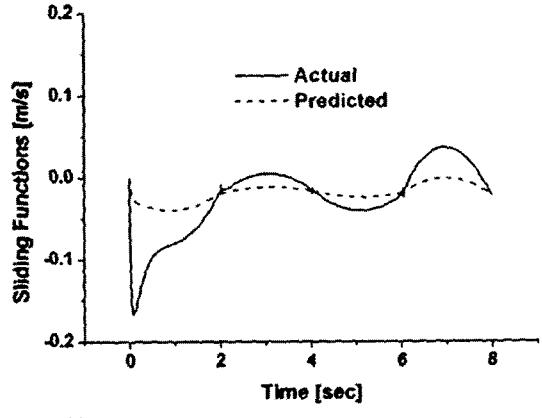

(f) Sliding surface of the robust controller

Fig. 7 Results of simulation of sliding mode control with sliding perturbation observer

good as shown in Fig. 7(a) (b).

Also, the chattering problem did not occur as shown in Fig. 7(c). The magnitude of the calculated nonlinear term is similar to the estimated perturbation term as shown in Fig. 7(d). In sliding surface of the robust controller, the predicted results are similar to actual ones. Also, the control performance is so good as shown in Fig. 8 in comparison of the estimated perturbation with compensation of the estimated perturbation term. Table 2 is the parameter for simulation.

Table 2 Parameter selections of simulation

Parameter	value
k_{1j}/ε_{oj}	60
k_{2j}/k_{1j}	20
α_{3j}	2.58
K_j/ε_{oj}	20
c_j	20
B_{eq}	2000
M_{eq}	100

4.3 Experimental results

In order to evaluate the proposed control algorithm, SMC is compared with SMCSPO. The control input of SMC is given by

$$u_j = \boldsymbol{I}\{-\boldsymbol{K}_j\, \boldsymbol{sat}(s_j) - \boldsymbol{c}_j\dot{\boldsymbol{e}}_j + \ddot{\boldsymbol{\theta}}_{dj}\} \qquad (27)$$

where $\boldsymbol{I}$ is the inertia matrix, $\boldsymbol{K}_j = diag[K_j]$ $(K_j > 0)$, $\dot{\boldsymbol{e}}_j = [\dot{e}_1 \cdot\cdot \dot{e}_6]^T$, $\boldsymbol{sat}(s_j) = [sat(s_1) \cdot\cdot sat(s_6)]^T$, and $\boldsymbol{\theta}_{dj} = [\theta_{1d} \cdot\cdot \theta_{6d}]^T$

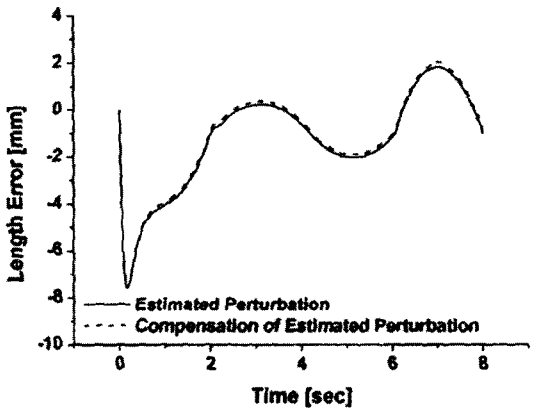

(a) Comparison of position error

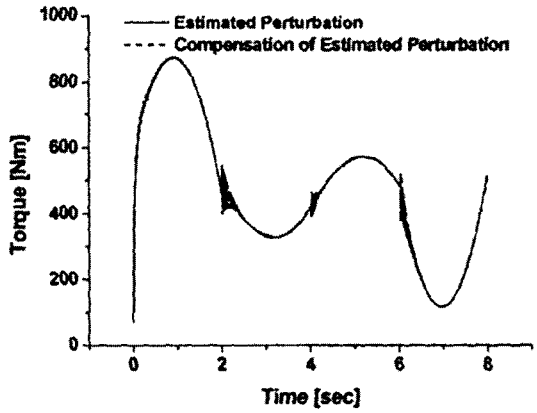

(b) Comparison of input torque

Fig. 8 Comparison of extimated perturbation with compensation of estimated perturbation

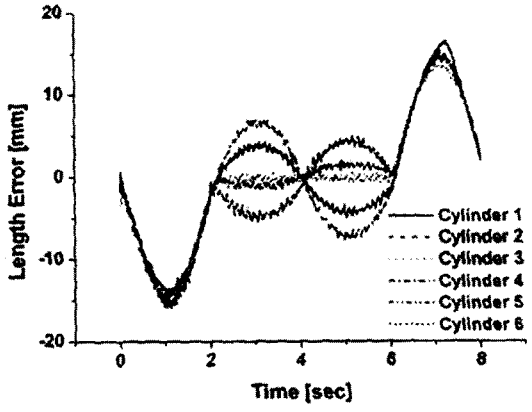

(a) Position tracking error

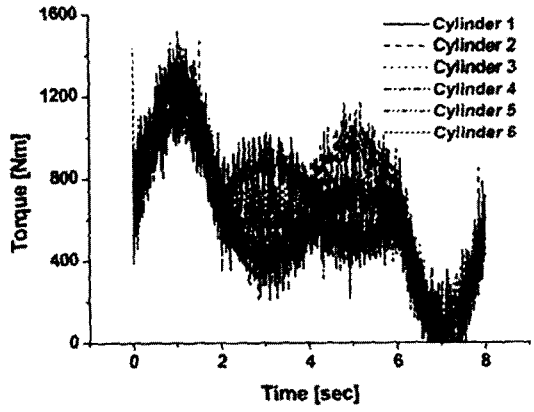

(b) Input torque of the system

Fig. 9 Results of experiment of sliding mode control

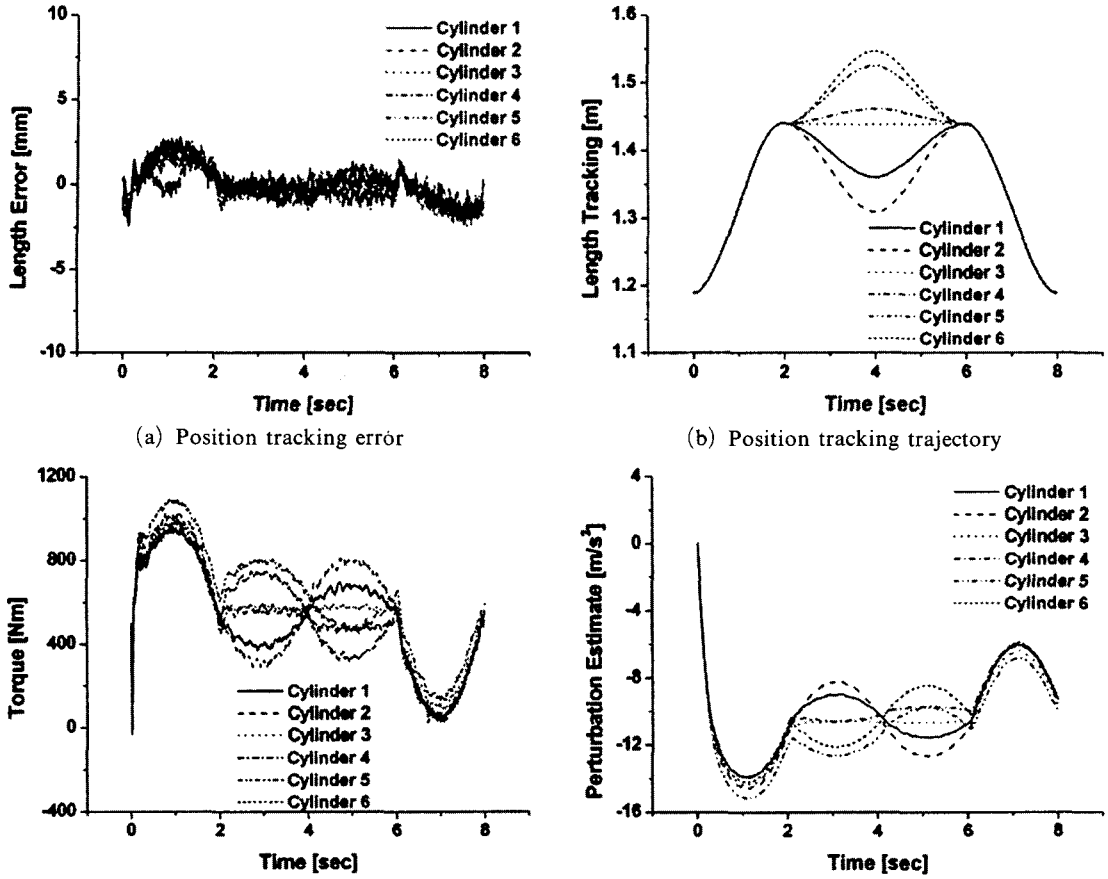

(a) Position tracking error

(b) Position tracking trajectory

(c) Input torque of system

(d) Perturbation estimate

Fig. 10 Results of experiment of sliding mode control with sliding perturbation observer

The control gains are selected as K_j=20.43 and c_j=20.43. The Stewart platform is used in experiment. The results of experiment of sliding mode control are shown in Fig. 9. The results of experiment of sliding mode control with sliding perturbation observer are shown in Fig. 10. The robust gain λ_d is same to the gain of the simulation using the genetic algorithm.

In the results of experiment of SMC, initial position tracking error is occurred within about 15 mm. However, the errors are converged within about 8 mm during roll motion in Fig. 9(a). Also, the problem of chattering is depicted in Fig. 9(b). Fig. 10 shows that SMCSPO yields better performance with less control activity.

The reason for this is the reduction of noise in the velocity feedback which appears in SMC. Fig. 10(a) shows that the position tracking errors are converged within about 1~2 mm. The performance of SMCSPO is superior to SMC.

5. Conclusions

This paper proposed a robust control algorithm for the Stewart platform and described gain optimization of the control algorithm. The proposed control algorithm can reduce the inherent chattering as estimating the states and compensating a perturbation in accuracy. The sliding perturbation observer is, therefore, proved to be superior to the conventional sliding observer. The performance of SMCSPO is shown to be limited by the dominant time constant of the control process. The optimal gains of SMCSPO are easily obtained by genetic algorithm. The proposed fitness function to optimize the gain is

defined using the sliding function. The simulation and experiment results show that SMCSPO can provide reliable tracking performance. This study is noticeable in that the same gains were used both in simulation and experiment. Moreover, the robust control algorithm does not require additional sensor in the system.

Acknowledgment

The authors would like to thank the Ministry of Science and Technology of Korea for financial support in the form of grant (M1-0203-00-0017-02J0000-00910) under the NRL (National Research Laboratory).

References

Stewart, D., 1966, "A Platform with Six Degree of Freedom," *Proc. of the Institute of Mechanical Engineering*, Vol. 180, pp. 317~386.

Hashimoto, H., Maruyama, K. and Harashima, F., 1987, "A Microprocessor-Based Robot Manipulator Control with Sliding Mode," *IEEE Trans. Industrial Electronics*, Vol. 34, No. 1, pp. 11~18.

Lee, M. C., Son, K. and Lee, J. M., 1998, "Improving Tracking Performance of Industrial SCARA Robots Using a New Sliding Mode Control Algorithm," *KSME Int. J.*, Vol. 12, No. 5, pp. 761~772.

Lee, M. C. and Aoshima, N., 1993, "Real Time Multi-Input Sliding Mode Control of a Robot Manipulator Based on DSP," *Proc. of SICE*, pp. 1223~1228.

Elmali, H. and Olgac, N., 1992, "Sliding Mode Control with Perturbation Estimation (SMCPE)," *International Journal of Control*, Vol. 56, pp. 923~941.

Slotine, J. J., Hedrick, J. K. and Misawa, E. A., 1987, "On Sliding Observers for Non-Linear Systems," *ASME Journal of Dynamic Systems, Measurement and Control*, Vol. 109, pp. 245~252.

Jairo Terra, M., Elmali, H. and Olgac, N., 1997, "Sliding Mode Control With Sliding Perturbation Observer," *Journal of Dynamic Systems, Measurement, and Control*, Vol. 119, pp. 657~665.

Park, M. K. and Lee, M. C., 2002, "Identification of Motion Platform Using the Signal Compression Method with Pre-Processor and Its Application to Sliding Mode Control," *KSME Int. J.*, Vol. 16, No. 11, pp. 1379~1394.